21

Passive Diplexers and Active Filters based on Metamaterial Particles

Daniel Segovia-Vargas[1], Vicente González-Posadas[2], José Luis Jiménez-Martín[2], Luis Enrique García-Muñoz[1] and Oscar García-Pérez [1]
[1] Universidad Carlos III de Madrid
Leganés-Madrid, Spain
[2] Universidad Politécnica de Madrid
Madrid, Spain

1. Introduction

Composite transmission lines are one of the main developments in the increasingly popular field of electromagnetic metamaterials, artificial electromagnetic structures with both negative electric permittivity and magnetic permeability (Caloz & Itoh, 2005). These structures present a backward wave or left-handed (LH) propagation instead of the conventional right-handed one. The first experimental microwave structures that presented this behavior were the result of combining thin wires and split-ring resonators (Shelby et al, 2001). Soon it was evident that narrow bandwidth operation and high losses were inherent to the resonant nature of this kind of metamaterials. In order to overcome the previous problems, some authors proposed the so-called metamaterial transmission lines or left-handed transmission lines LH TL (Sanada et al, 2004). The LH TL concept has been extended and generalized to the concept of composite right/left handed (CRLH) structures where mixed contributions of LH and RH cells occur in practice. More specifically, the CRLH transmission lines have become a very commonly used solution to obtain metamaterial properties with low losses and broader bandwidth. Then, below a certain frequency, a CRLH transmission line behaves as a left-handed transmission line while over higher frequencies it is basically a conventional right handed line. As a consequence of this combined behaviour, the phase response is not linear with respect to the frequency.

From the circuit application point of view, the two main characteristics of the CRLH transmission lines consist on obtaining miniaturized and/or dual band circuits. Then, it can be mentioned that dual band hybrid couplers (Lin et al, 2004), branch-line couplers (Keung & Cheng, 2004), dual-performance rat-race couplers (Castro-Galan et al, 2009) and enhanced rat-race couplers (Okabe, Caloz & Itoh 2004). The most critical aspect in the design of combiners, filters or diplexers with conventional CRLH transmission lines is the losses associated to them.

For the case of diplexers, using of the so called dual composite right left handed (D-CRLH) cells may overcome some of the previously stated problems. The D-CRLH transmission lines are the dual part of the CRLH transmission lines and were first proposed in (Caloz, 2006). Thus, this type of line presents a RH performance at low frequencies while LH at higher frequencies. From its equivalent circuit point of view, the D-CRLH section changes an equivalent bandpass of the CRLH section by a bandstop section. This is particularly useful in the design of diplexers. The design of a diplexer based on CRLH lines has shown drawbacks coming from the losses at the pass bands. A diplexer can be based either on allowing some frequency pass-bands or on rejecting the frequency stop-bands. The use of D-CRLH transmission lines can help to overcome the previous problems by working with the complementary rejection frequency bands. The design of microwave diplexers based on using of D-CRLH lines is presented in this chapter.

In addition, in order to avoid losses, the use of dual frequency active filters is also proposed. This dual-frequency performance can be achieved by making use of conventional CRLH transmission lines. The inclusion of this type of lines as feedback sections in a first order recursive topology can be used to generate a filtering response with two arbitrary pass bands. Additionally, dual-band couplers are also required. These may be implemented by means of CRLH structures or by shunted stub branch line structures. This second structure produces a strong rejection level at the central stop band what improves the overall response of the dual frequency active filter. Theoretical analysis and design procedures are verified by means of manufacturing and measurement of a prototype.

Then, passive diplexers based on D-CRLH lines and dual frequency active filters based on conventional CRLH transmission lines are presented in this chapter.

2. Dual Composite Right-Left Handed transmission line theory

The D-CRLH structure, shown in Fig. 1, behaves as the complementary structure of the conventional CRLH cell. This unit cell has a series parallel LC tank circuit and a shunt series LC tank. The D-CRLH indeed exhibits its left-handed band at high frequencies and its right-handed band at low frequencies and is of stop-band nature.

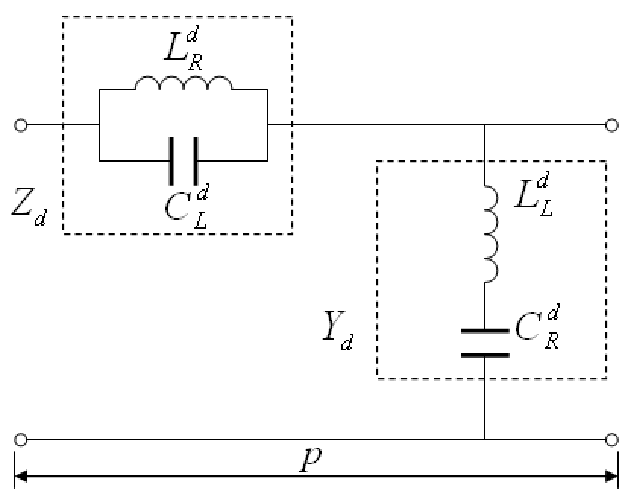

Fig. 1. Schematic of the D-CRLH Transmission Line

The equations running the performance of the D-CRLH balanced line are given in (1)-(3). If the resonance frequencies of the shunt LC tank and the series LC tank were w_{sh} and w_{se} a balanced condition could be achieved by satisfying (1)

$$\omega_0 = \sqrt{\omega_{sh} \cdot \omega_{se}} \tag{1}$$

Once the D-CRLH line is balanced, if a right and left cut-off frequencies are defined, then it can be written that

$$\omega_R = \sqrt{\frac{1}{L_R \cdot C_R}}; \omega_L = \sqrt{\frac{1}{L_L \cdot C_L}} \tag{2}$$

The characteristic impedance of the line is given by

$$Z_0 = Z_R = Z_L = \sqrt{\frac{L_R}{C_R}} = \sqrt{\frac{L_L}{C_L}} \tag{3}$$

Finally, the propagation constant is given by

$$\beta(\omega) = \frac{1}{\frac{1}{\beta_R} + \frac{1}{\beta_L}} = \frac{1}{\frac{1}{\omega/\omega_R} + \frac{1}{\omega_L/\omega}} = \frac{1}{\frac{\omega_R}{\omega} - \frac{\omega}{\omega_L}} = \frac{\omega_L \cdot \omega}{\omega_0^2 - \omega^2} \tag{4}$$

The stop-band frequencies can be computed from the local impedance by placing two cutting-off frequencies, one in the left-handed part and other at the right-handed one. These cutting-off frequencies are given by the following equation

$$\omega_{CL/R} = \omega_0 \cdot \sqrt{1 + \frac{\omega_L}{8 \cdot \omega_R} \pm \sqrt{\frac{\omega_L}{4 \cdot \omega_R} + \sqrt{1 + \frac{\omega_L}{16 \cdot \omega_R}}}} \tag{5}$$

where the sign + is for the left handed high-pass cutoff and the sign - is for the right handed low-pass cutoff. It must be noted that $\omega_{CL} > \omega_{CR}$.

Fig. 2 (taken from (González-Posadas et al, 2008)) shows the performance of a dual-CRLH line, both in amplitude and phase with the band-stop at 970 MHz. It can be seen that the structure presents a rejection bandwidth instead of a passing one (as it would be for the conventional CRLH case).

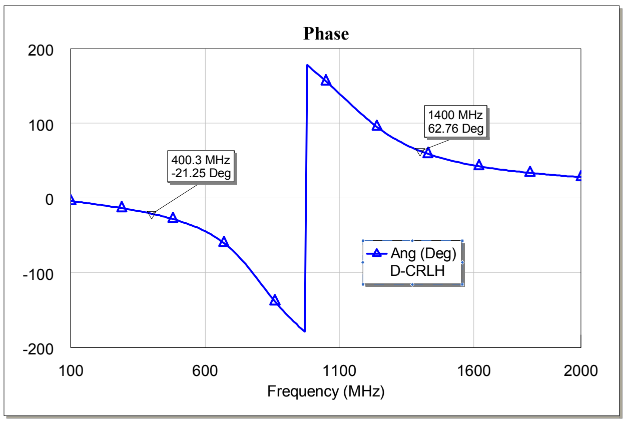

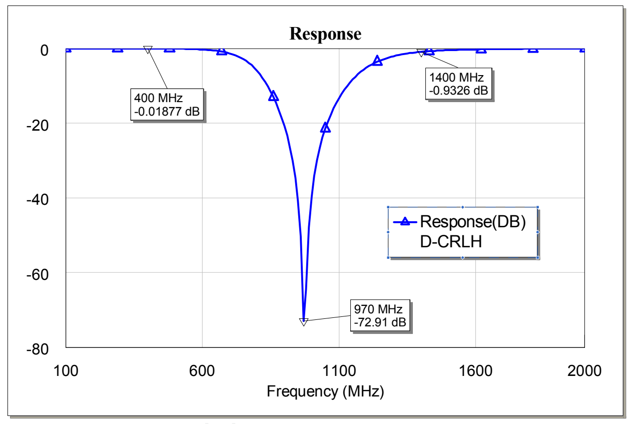

Fig. 2. D-CRLH Phase (left) and amplitude (right) response. The parameter are L_R=6 nH, C_R=4.452 pF, L_L=11.13 nH, C_L=2.4 pF.

3. Passive diplexer design

In this section the principles for the diplexer design based on D-CRLH lines will be presented. A generalization for a multistage diplexer design will be also given. Finally, some experimental results will be shown to prove the validity of the proposed design strategy.

3.1 Design principles

The realization of diplexers with CRLH lines has not shown a great development till now. Different topologies to build CRLH diplexers have been used. In all these cases the CRLH transmission line was used to allow the desired frequency band and reject the non-desired one. In this way, all the problems associated with the sensitivity and losses of the CRLH transmission lines were present. Then, (Bonache et al, 2005) used split-ring-resonators for a classical diplexer topology; (Horii, Caloz & Itoh, 2005) proposed a vertical topology to achieve a very compact diplexer at a price of large losses and a frequency shift; finally, (Wong, Balmain & Eleftheriades, 2006) proposed an original and non-compact planar topology for diplexer design.

The dual performance of the so called D-CRLH transmission lines allows a different design strategy for diplexers. The strategy is based on rejecting the non-desired frequency bands instead of allowing the desired ones. In this way, the diplexer design will be based on working with D-CRLH transmission lines tuned at the frequency that is not allowed. Thus, the band-stop performance of a D-CRLH line is used to design a diplexer. Then, for a diplexer separating the frequencies f_1 and f_2 (being $f_1 < f_2$), the first D-CRLH line, according to Fig. 3, has a stop-band at f_1 and a pass band at f_2; however, the second D-CRLH line presents a stop-band at f_2 and a pass band at f_1. From the left and right handed performance of the corresponding D-CRLH lines, it can be seen that the first D-CRLH line is left-handed at the higher passing frequency (f_2) while the second D-CRLH line is right-handed at the lower passing frequency (f_1), just the opposite as it would be for the conventional CRLH transmission line. In this way, any of these D-CRLH lines will be used in any of the branches of the proposed diplexer.

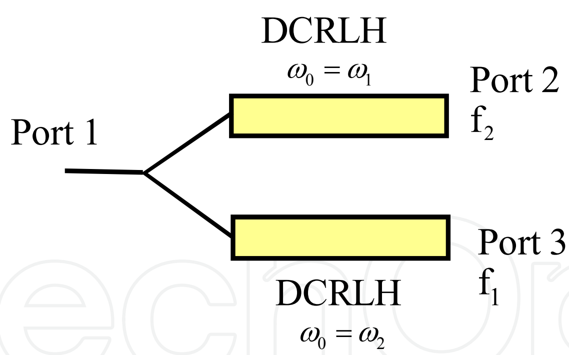

Fig. 3. Proposed D-CRLH diplexer structure

The design frequency has been chosen as the non-desired frequency (f_1 for the band allowing f_2 pass, say port 2 in the Fig. 3, and f_2 for the band allowing f_1 pass, say port 3 in Fig. 3). Let us introduce a factor $k(N)$, being N the number of cells of the D-CRLH transmission line, as the one that defines the ratio between the band stop frequency and the cutting-off frequencies of the D-CRLH lines. This factor depends on the number of cells in the D-CRLH line and on the frequency separation and will define two cutting-off frequencies: towards its right corresponding to the left-handed performance and towards its left corresponding to its right-handed performance. Without loss of generality, let us assume that the number of cells is 1 for the following design procedure.
First, choice of the band-stop frequencies for the two balanced D-CRLH structures. These frequencies are chosen in a way that the corresponding central frequency is the one allowing the other frequency pass

$$\omega_1 = \omega_{lower}; \omega_2 = \omega_{higher}; \omega_2 > \omega_1 \tag{6}$$

Secondly, define the right-handed cutting-off frequency of the D-CRLH section centred at ω_2 and the left-handed cutting-off frequency of the D-CRLH section centered at ω_1. Then, for the D-CRLH that allows passing the low frequencies the phase must be positive, that is right-handed, and left-handed for the line that allows passing the high frequency

$$\omega_{1cL} = \omega_{lower} \cdot k(N); \omega_{2cR} = \frac{\omega_{higher}}{k(N)} \tag{7}$$

The values for the right and left cutting off frequencies are, then, given as

$$\omega_{CL/R} = \omega_0 \cdot \sqrt{1 + \frac{[k(N)]^2}{8} \pm \sqrt{\frac{[k(N)]^2}{4} + \sqrt{1 + \frac{[k(N)]^2}{16}}}} \tag{8}$$

If the ratio between the higher and lower frequency is called R, a graphical representation between the value R and the factor $k(N)$ can be obtained. This ratio is given in Fig. 4.

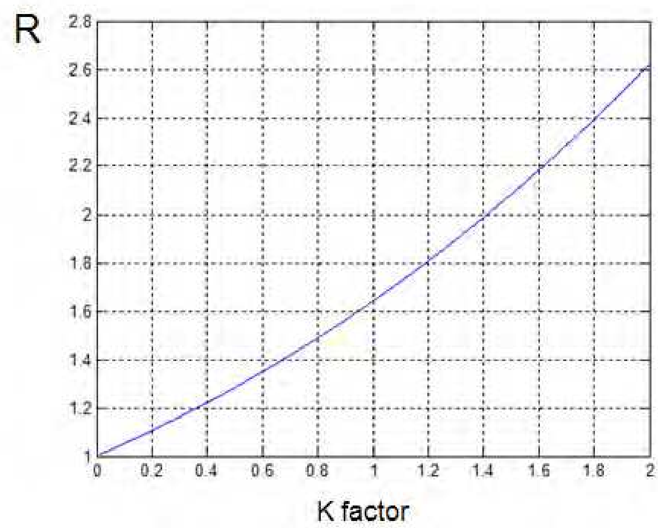

Fig. 4. *K* factor as a function of the ratio R between the higher and lower frequency

Once the value of the *k* factor and of the frequency ratio *R*, has been determined, the values for each branch left-handed and right-handed capacitors can be found out as follows. Thus for the branch rejecting the lowest frequency and allowing the highest one (port 2 in Fig. 3), the values for the components are given as

$$L_{1R} = \frac{Z_0 \cdot k(N)}{\omega_{lower}}; L_{1L} = \frac{Z_0}{\omega_{lower} \cdot k(N)}; C_{1L} = \frac{L_{1L}}{Z_0^2}; C_{1R} = \frac{L_{1R}}{Z_0^2} \tag{9}$$

And for the branch rejecting the highest frequency and allowing the lowest one (port 3 in Fig. 3), the values for the components are given as

$$L_{2R} = \frac{Z_0 \cdot k(N)}{\omega_{higher}}; L_{2L} = \frac{Z_0}{\omega_{higher} \cdot k(N)}; C_{2L} = \frac{L_{2L}}{Z_0^2}; C_{2R} = \frac{L_{2R}}{Z_0^2} \tag{10}$$

3.2 Multistage diplexer

For the general case where the number of cells is *N* (larger than 1), the values of the components are given by the following expressions

$$L_{1,2R,N} = \frac{L_{1,2R}}{N}; L_{1,2L,N} = L_{1,2L} \cdot N; C_{1,2R,N} = \frac{C_{1,2R}}{N}; C_{1,2L,N} = C_{1,2L} \cdot N \tag{11}$$

A discussion on the number of sections and on the D-CRLH performance can be done now. In (Caloz, 2006) the D-CRLH performance was proven for a 10-cell transmission line structure. If the number of cells is reduced the left-handed performance still maintains as it has been shown in (Herraiz et al, 2007). The only dependence on the number of cells to be implemented comes from the fact that the transient response between the low frequency right-handed region and the high-frequency left-handed one is more abrupt when the number of cells is larger. However, from the diplexer design point of view a trade-off between the desired losses and the rejection factor at the non desired frequency in the corresponding branch must be considered. In this way, for most single designs low orders (1 or 2) for the identical D-CRLH sections are enough to achieve the desired performance. Next section will show the design of a particular one-stage or multistage diplexer.

3.3 Experimental results

Since one of the most important features is its miniaturization, the presented design procedure will be applied to the low microwave frequency band, to separate frequencies working at TETRA-GSM bands (380 MHz and 960 MHz). As the working frequencies are far enough, initially a one stage design will be taken into account. The schematic of the proposed diplexer is shown in Fig. 5. (AWR ®). For this diplexer, the value for the factor *k(N)* is 2.01. The conventional transmission lines allow joining the two branches and soldering the SMA connectors and, at the same time they are optimized to achieve the lowest return losses. The proposed circuit has been implemented on an Arlon600 substrate with a relative permittivity of 6, height of 0.6mm.

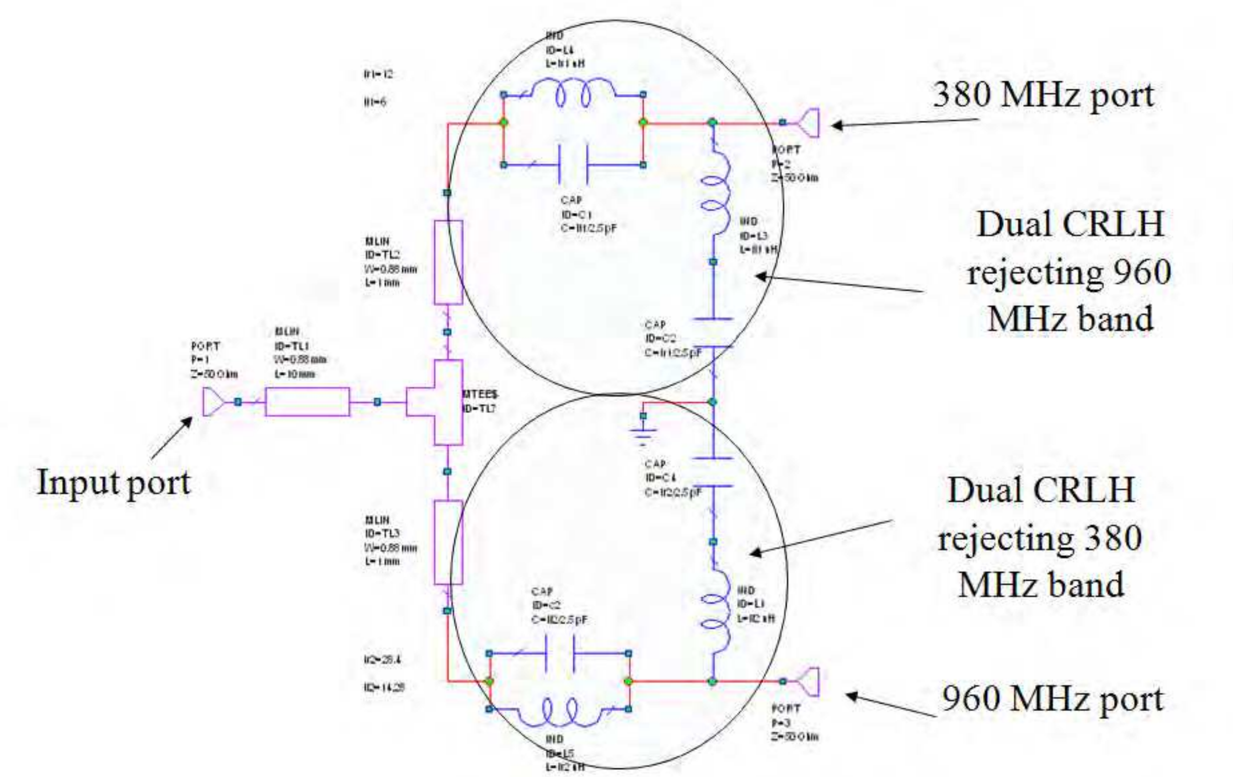

Fig. 5. Schematic of the one stage diplexer for separating TETRA and GSM frequencies.

The simulated transmission parameters (in dB) of any of the two branches are shown in Fig. 6. It can be seen that the upper part in the schematic of Fig. 5 corresponds to the s_{31} parameter in the transmission parameter of Fig. 6 since it rejects the 960 MHz band and allows the 380 MHz band. In the same way, the lower part corresponds to the s_{21} parameter.

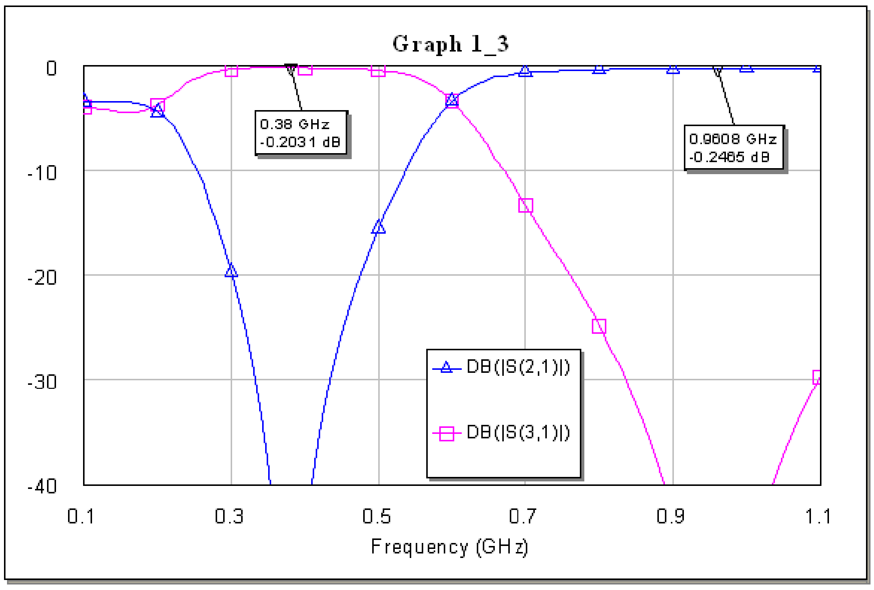

Fig. 6. Transmission parameters of any of the two diplexer branches

For the case presented before it can be seen that the simulated losses in the desired bandwidths (around 0.2 dB at any frequency) and the rejection parameter at the non desired frequency (lower than 40 dB) are enough for a good performance of the diplexer. If the diplexer frequencies were closer or a steeper slope would be needed a larger number of sections would be required. Fig. 7 shows a comparison between the transmission parameters (s_{31} and s_{21}) for a diplexer made with one D-CRLH cell (as in the previous case) and other diplexer made with four D-CRLH cells. It can be seen that the main difference is the slope of the rejection bandwidth. For the proposed example it can be seen that the number of sections can be done as low as possible, then the number of sections will be equal to 1.

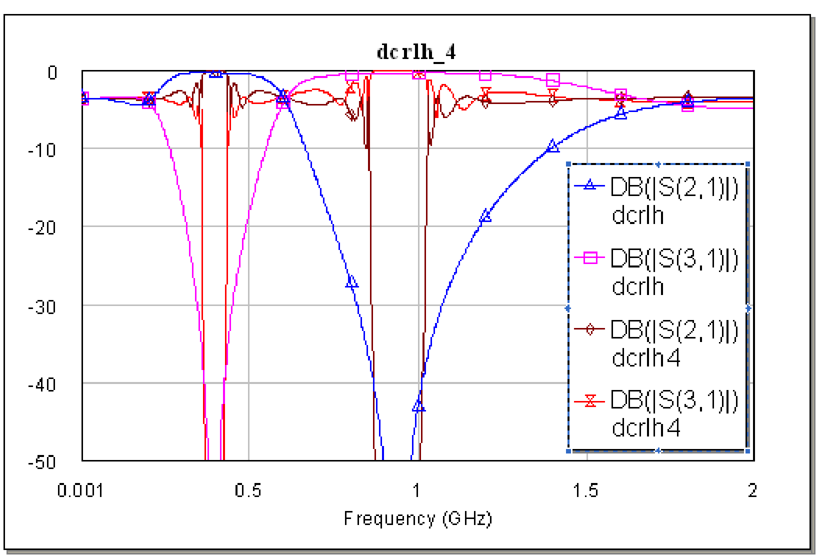

Fig. 7. Comparison between the transmission parameter for the previous one-D-CRLH-cell structure and a four-D-CRLH-cell structure.

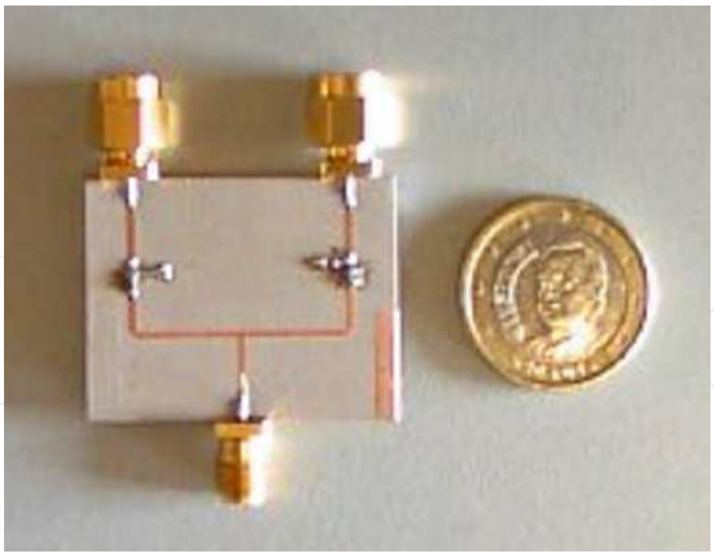

Fig. 8. Photo of the proposed one-cell D-CRLH diplexer.

Finally, a prototype has been manufactured and measured. Fig. 8 shows a photo of the manufactured prototype. Fig. 9 shows the transmission and reflection measurement of the manufactured one-cell diplexer. The measurements show an excellent agreement with simulation. In addition, the insertion losses are lower than 0.4 dB at both frequency bands. The return losses are lower than -22 dB at each frequency band and at any diplexer port. Lastly the isolation between the two output ports is nearly 40 dB at both working frequencies. In addition, the compactness of the circuit is quite good and miniaturization has achieved for a diplexer circuit working in the UHF frequency bands.

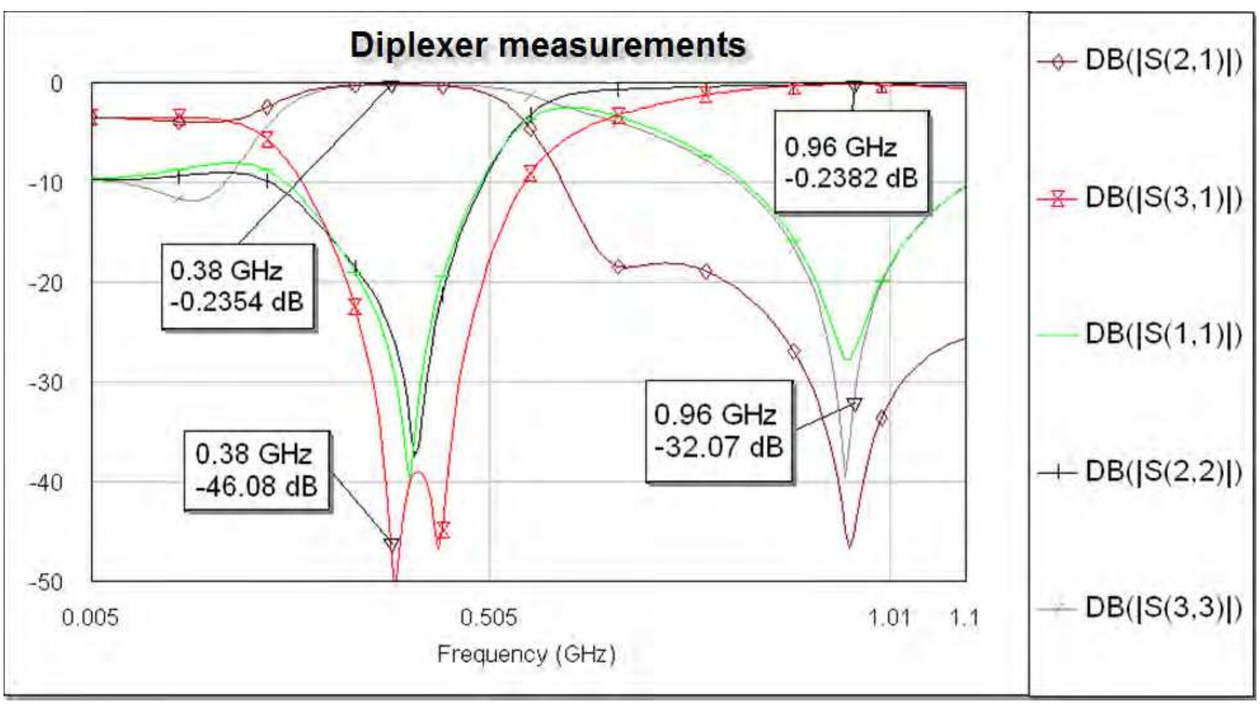

Fig. 9. Measurements of the transmission and reflection parameter for the one-cell D-CRLH diplexer.

4. Principles of active filters based on metamaterial cells.

One way of reducing the filtering losses is by means of active filters. The most usual microwave active filters can be classified into four main groups: filters based on negative resistance elements (Chang et Itoh, 1990), based on active inductors (Lucyszyn & Robertson, 1994), transversal, and recursive filters (Rauscher, 1985). In opposition to the first types, based on lumped elements, the two last ones are distributed filters, and therefore more adequate for high-frequency applications. The frequency selective response is generated by means of a combination of signal components that propagate along several electrical sections with different amplitudes and phase delays. The single difference between both schemes is that the transversal type only needs feed-forward branches, whereas the recursive one also includes feedback. This last approach is chosen as it is usually easier to design and produces more compact structures (the number of junction elements that occupy a large part of the total layout area, is in general smaller) (Rauscher, 1985). Of course, potential instability issues related to the feedback must be addressed (Billonet, Jarry & Guillon, 1995), but this is true for every microwave network that contains active elements, as they always show parasitic feedback.

The filtering characteristic of a first order recursive filter is generated by combination of the main path signal component with a properly weighted and delayed sample of the output of the network, which constitutes the feedback. The key of this process is therefore the phase response of the feedback section that must have certain value at the center frequency of the pass band. Thus, it can be implemented by means of a transmission line section. The objective is to extend the operation of recursive active filters to dual pass band frequency responses. In order to produce a dual-band response, the phase condition should be fulfilled at two different, controllable frequencies, and for this reason conventional transmission lines are not suitable. In fact, the solution proposed makes use of composite right/left-handed (CRLH) transmission lines (García-Pérez et al, 2009).

4.1 Theoretical design

Theoretical concepts of microwave active recursive filters derive from low frequency and discrete-time filtering techniques. An example of a first-order digital filter and its equivalent microwave recursive filter is shown in Fig. 10. In that figure *x(t)* and *y(t)* denote the time-dependent input and output signals respectively, a_0 and b_1 are gain weights, and τ represents a time delay. The frequency transfer function is given as

$$H(f) = \frac{Y(f)}{X(f)} = \frac{a_0}{1 - a_0 \cdot b_1 \cdot e^{-j \cdot 2\pi \cdot f \cdot \tau}} \tag{12}$$

The transfer function *H(f)* describes a periodic band-pass filter response. The center frequency of each band, f_0, is characterized by the total phase response of the loop Φ_{loop} being a multiple of 2π

$$\Phi_{loop} = -2\pi \cdot f \cdot \tau = -n \cdot 2\pi \Rightarrow f_0 = n \cdot 1/\tau\,, \tag{13}$$

where n denotes any integer number. Therefore, for those frequency values f_0, the signal coming from the feedback branch is combined in phase with the input signal, resulting in maximum gain values.

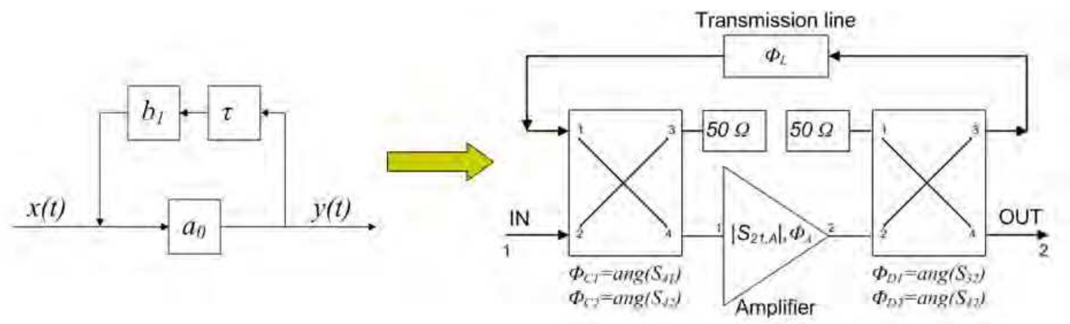

Fig. 10. Flow graph of a first order digital filter and equivalent microwave recursive active filter.

Although recursive filters of any order are possible, the most common cases are first-order topologies because of their simplicity. Of course, in order to fulfill stricter requirements of bandwidth or in-band ripple, higher order structures may be needed. However, the study presented here will be restricted to the simpler first order networks. The scheme presented in the left part of Fig. 10 can be transformed into a microwave filter circuit just by replacing all its parts with microwave components resulting in the right part of Fig. 10. For example, the time delay τ is implemented by means of a transmission line section while the weight coefficient a_0 corresponds to an amplifier. Also, the signals have been combined at the input/output ports by using branch-line couplers as combiners/dividers. Their power ratios can be absorbed into the term b_1.

In this context, the band-pass center frequencies from (13) are the values f_0 for which the loop phase condition is satisfied,

$$\Phi_{loop} = \Phi_A(f_0) + \Phi_{D1}(f_0) + \Phi_L(f_0) + \Phi_{C1}(f_0) = -n \cdot 2\pi \tag{14}$$

where $\Phi_A(f_0)$, $\Phi_{D1}(f_0)$, $\Phi_L(f_0)$ and $\Phi_{C1}(f_0)$ denote the phase responses of the amplifier, the power divider, the transmission line section and the power combiner respectively, all of them obtained at the band-pass frequency f_0, being n an integer number. Therefore, in the same way as the previous case, each operating frequency f_0 can be seen as the frequency at which the signal from the feedback transmission line is combined constructively (i.e.: with null relative phase shift) with the input power signal. This condition can be ensured by enforcing the loop phase to be multiple of 2π.

If the combiners were implemented with 3 dB combiners or power dividers then, if the filter gain function $|s_{21,F}(f_0)|$ were represented in front of the amplifier gain $|s_{21,A}(f_0)|$, two distinct operation zones could be observed (sub index $_F$ denotes filter while sub index $_A$ denotes amplifier). The first one corresponds to $|s_{21,A}(f_0)|$ under 6 dB, where $|s_{21,F}(f_0)|$ grows up with $|s_{21,A}(f_0)|$; in the second one $|s_{21,A}(f_0)|$ is over 6 dB and $|s_{21,F}(f_0)|$ decreases with it. There exists a value of the amplifier gain below which the circuit is unconditionally stable. That is $|s_{11,F}(f_0)|<0$ dB, at every frequency and for every combination of phases in the loop. This value corresponds to $|s_{21,A}(f_0)|=3.5$ dB when using 3 dB branch line couplers, but may take other values if different power combiners are used. From this value up to $|s_{21,A}(f_0)|=6$ dB the filter behaves as potentially unstable. For higher values ($|s_{21,A}(f_0)|>6$ dB) the circuit has been analytically demonstrated to be unconditionally unstable (Billonet, Jarry & Guillon, 1995) and (García-Pérez et al, 2009).

4.2 Requirements for dual band operation

Some important conditions must be addressed in order to design dual-band recursive filters. Firstly, the phase equation (14) must be simultaneously satisfied at both filtering frequencies. Since the phase delays introduced by the amplifier (Φ_A) and the power combiners (Φ_{D1}, Φ_{C1}) are fixed once those components are chosen, the only design variable is the phase delay of the feedback transmission line (Φ_L). For conventional single-band filters only one condition is imposed at the design frequency and, therefore, it can be fulfilled by choosing the correct length of transmission line. However, for dual-band responses two different conditions should be established and, in general, the linear phase delay exhibited by conventional transmission lines is not enough to simultaneously meet both of them. The inclusion of CRLH transmission lines as feedback lines is proposed, since their non-linear behavior provides more degrees of freedom. The second condition is that power combiners working simultaneously at both design frequencies are indispensable. They have a double purpose: obtain a good input/output match at the operating frequencies and isolate the input port with respect to the power coming from the feedback line avoiding stability problems, which are critical when working with feedback topologies.
The phase response exhibited by the whole CRLH transmission line at frequency f can be expressed as

$$\Phi_{CRLH}(f) = 2 \cdot \Phi_{RH}(f) + N \cdot \frac{1}{2\pi \cdot f \cdot \sqrt{L_L \cdot C_L}} \tag{15}$$

where Φ_{RH} denotes the phase response of each transmission line section, N is the number of left handed T-cells, and L_L and C_L denotes the values of the lumped inductors and capacitors.
Usually, the phase delay given by a power combiner takes a fixed value at its operating frequencies, so (14) can be reduced to an expression only dependent with the phases of the transmission line section (Φ_L) and the amplifier (Φ_A). Since the phase delay of a branch line coupler is Φ_{C1}=Φ_{D1}=π rad, the phase condition in (14) when using branch line couplers can be expressed as

$$\Phi_L(f) + \Phi_A(f) = -n \cdot 2\pi, \;\; f = f_1, f_2 \tag{16}$$

where n can take any integer value, and f_1 and f_2 are the two desired band-pass frequencies. By substituting $\Phi_L(f)$ with the phase of a CRLH transmission line from (16), a system of two simultaneous equations is established. Its solutions (lengths of transmission line sections, number and values of lumped elements) constitute the design parameters used for the prototypes in next section.
Concerning the branch-line couplers two possible solutions could be available: dual frequency branch line couplers with CRLH lines (Lin et al, 2004) or dual frequency branch line couplers with parallel stubs fulfilling the branch line design equations (Cheng & Wong, 2004). The CRLH line-based solution has an important drawback with respect to the stub-loaded branch line. Apart from its complexity and the parasitic effects of the lumped elements, the CRLH line-based solution does not show transmission zeros at the intermediate band between the pass bands resulting in an overall spurious bands in the active filter (this will be shown in the next subsection of experimental results). For that reason this solution is discarded.

The second alternative shows a transmission zero located at the frequency halfway between the pass bands, for which the stubs behave as short circuits. As a result, rejection can be highly increased at the inner stop band. This is especially important if condition (14) is verified at the two pass bands for non-consecutive multiples of 2π, since spurious pass bands are also generated between them, in the stop band. The filtering characteristic of the branch line can be used to eliminate or at least mitigate these undesired transmission spikes. For that reason, this will be solution chosen.

4.3 Experimental results

In order to test the feasibility of the dual band recursive active filters described in the previous sections two prototypes have been designed and built: one with a CRLH branch line (that will be finally discarded) and other with parallel stubs branch line coupler.

4.3.1 Active filter with CRLH branch coupler

The first active filter has its pass bands centered at f_1=0.9GHz and f_2=1.6GHz, uses branch line couplers implemented with CRLH transmission lines as combiners. In order to reduce the total size of each combiner, a new modification has been introduced in their design that consists of placing two Schiffman lines sections at each horizontal branch of the hybrid, close to the left-handed sections. Each Schiffman section is a pair of coupled transmission lines which can be designed to be equivalent to a conventional transmission line, but needing less space. The result is a significant reduction of one of the two dimensions of each power combiner, and therefore of the whole circuit footprint. The active stage will be composed of the monolithic amplifier ERA-5+ of Mini-Circuits®. It is necessary to add an attenuator in series to maintain the gain under 6dB, in order to avoid instabilities.

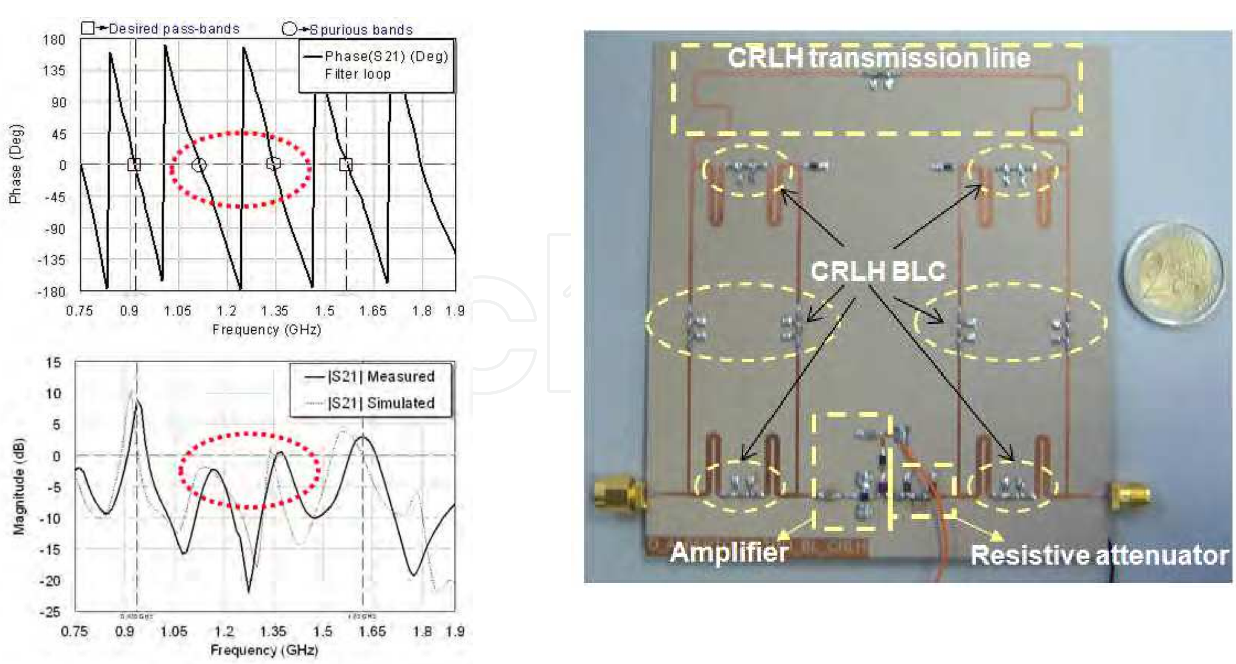

Fig. 11. Left part, phase response of the active filter showing the desired bands and the spurious ones. Right part, photo of the prototype with CRLH lines and Schiffman lines.

From Fig. 11 it can be seen that although the feedback CRLH line has been designed as electrically short as possible, the contributions in phase of the branch line coupler makes unavoidably the loop to be a section electrically long. This makes the phase condition to be fulfilled at undesired intermediate frequencies. The effect is the appearance of spurious pass bands as can be seen in Fig. 11. These undesired spurs at intermediate frequencies, between both desired pass bands, at 1175MHz and 1370MHz, are caused by the feedback loop phase response, that takes values near to a multiple of 2π rad. Then, the signal coming from the feedback line is constructively added at the input. These spurs, which appear out of the frequencies at which the hybrids are designed, are mitigated by the own transfer function of the hybrids, but are difficult to eliminate since the hybrid does not present a rejection band. For that reason this topology is discarded as a suitable one to achieve dual-band active filters.

4.3.2 Active filter with shunted stubs CRLH branch coupler

Another prototype has been designed and built with its pass bands centered at f_1=0.8 GHz and f_2=1.7 GHz. The shunted stubs branch line couplers present a more compact layout with very high rejection level between the pass bands. With regard to the active stage a single-stage distributed amplifier has been used to achieve a flat gain response over both band-pass frequencies. A resistive network has also been included to avoid instability problems. All these elements can be seen in Fig. 12.

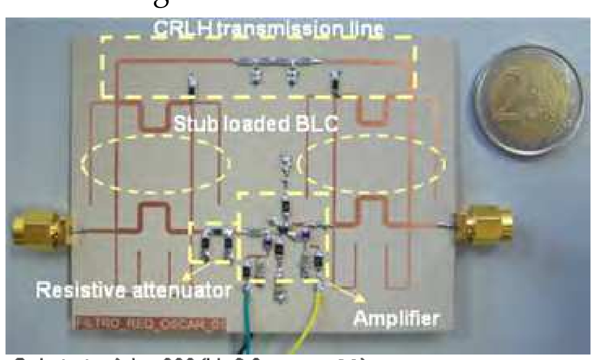

Substrate: Arlon 600 (H=0.6mm, εr=6.2)

Fig. 12. Photo of the prototype with shunted stubs branch line coupler

The feedback CRLH transmission line has been designed to fulfill two conditions: first, its phase response must satisfy (14) and, second, the equivalent characteristic impedance must be 50 Ω. Once again, although the feedback line has been designed as electrically short as possible, the complete phase loop including all the components delays is electrically long, and spurious bands appear unavoidably. Thus, two spike-shaped spurious pass bands appear at the inner stop band, corresponding to the non-desired solutions. Although non-desired solutions appear, they are cancelled out due to the high signal rejection introduced by the couplers in both the main path and the feedback loop. As stated before, this rejection is produced by the zero of the transmission and coupling coefficients associated with the branch-line port stubs. The amplitude response of the shunted branch line coupler can be seen in Fig. 13 where a strong rejection band appears between the two desired bands.
Due to this rejection band the two spikes closer to the pass bands are highly attenuated and have a reduced effect, with a transmission level of -8 dB at 1025 MHz and -6 dB at 1470 MHz. This can be seen in the overall response of the active filter that is shown in Fig. 14. The

upper part shows the phase response where the desired and spurious frequencies have been marked. It can be seen that two desired bands at 800 MHz and at 1700 MHz appear. However, three other spurious bands appear at 1025 MHz, 1175 MHz and 1470 MHz.

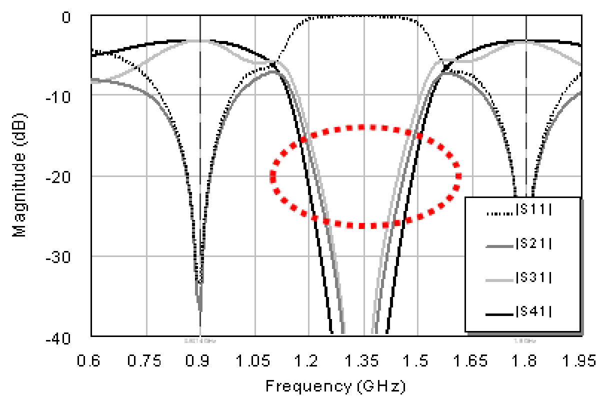

Fig. 13. Amplitude response of the shunted stubs branch line coupler.

The overall filter amplitude response is seen in the bottom part of Fig. 14. Due to the rejection of the branch line coupler the spurious band at 1175 MHz is completely rejected at levels lower than -30 dB. The other two spurious bands at 1025 MHz and 1470 MHz are also rejected presenting transmission levels lower than -6 dB. For that reason this topology for dual band active filters can be considered as suitable and will not be discarded as the previous one.

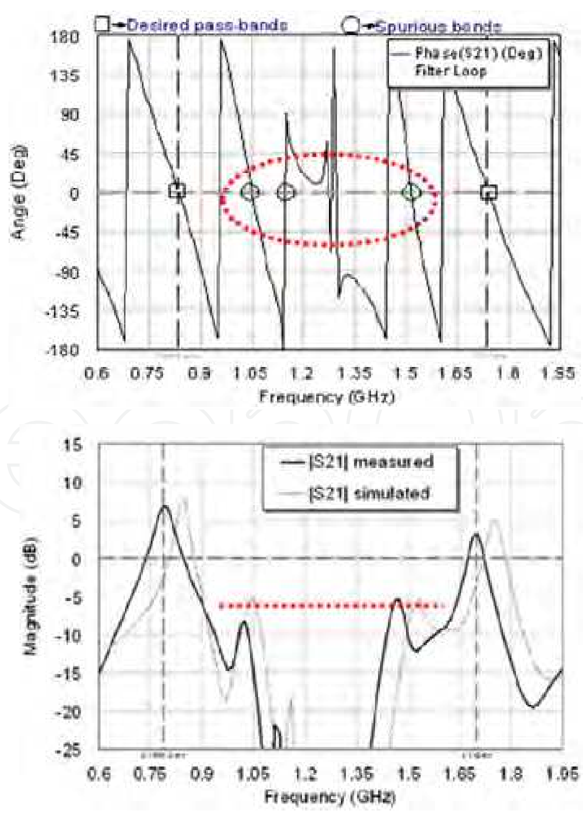

Fig. 14. Upper part, phase and amplitude response of the active filter showing the desired bands and the spurious ones (from García-Pérez et al, 2009).

5. Conclusion

This chapter is devoted to obtaining filtering and diplexing structures with losses as low as possible. First dual composite right/left handed cells have been proposed to reduce the losses; secondly active structures have been proposed to achieve dual band active filters.
The first part of the chapter is devoted to D-CRLH transmission lines as a good solution for the design of circuits that are alternatively used for rejecting or allowing different frequency bands. Then, a D-CRLH diplexer-circuit based on D-CRLH transmission lines has been proposed. A general design procedure for implementing arbitrary-frequency compact diplexers has been proposed. As the D-CRLH transmission lines de not present a frequency periodic performance, the proposed diplexer can be designed for every given frequency ratio f_2/f_1.
The second part of the chapter is devoted to the design of dual band active filters. A theoretical study describing the principles of this type of filters is developed through the text. Since the proposed scheme uses feedback sections, stability matters have to be taken into account. In this way, it may be necessary to limit the amplifier gain by adding attenuators in the active stage. Another important issue is the appearance of undesired spurious peaks at frequencies in the inner band. In order to mitigate their effect, branch-line couplers with shunted stubs are used to provide dual band operation and strong rejection between the pass-bands.

6. References

Caloz, C & Itoh, T. Electromagnetic Metamaterial Transmission Line Theory and Microwave Applications, IEEE Press and Wiley, ISBN 0471-66985-7, New York, , 2005.

R. A. Shelby, D. R. Smith & S. Schultz. Experimental verification of a negative index of refraction. Science, vol. 292, April 2001, pp. 77-79, ISSN 0036-8075.

Sanada, A.; Caloz, C. & Itoh, T., Characteristics of the composite right/left-handed transmission lines, IEEE Microwave and Wireless Component Letters, vol. 14, no. 2, Feb. 2004, pp. 68–70, ISSN 1531-1309.

I-Hsiang Lin, M. de Vicentis, C. Caloz, T. Itoh; Arbitrary Dual-Band Components Using Composite Right/Left-Handed Transmission Lines", IEEE Trans. On Microwave Theory and Techniques, vol. 52, no. 4, April 2004, pp. 1142-1149, ISSN 0018-9480.

K. Keung, M. Cheng; A Novel Approach to the design and implementation of dual-band compact planar 90 branch-line coupler", IEEE Trans. On Microwave, Theory and Techniques, vol. 52, no 11, November 2004, ISSN 0018-9480.

D. Castro-Galan, L. E. Garcia-Muñoz, D. Segovia-Vargas and V. Gonzalez-Posadas, Diversity monopulse antenna based on a dual frequency and dual mode CRLH rat-race coupler, Progress in Electromagnetic Research, PIERB, 2009, vol.14, pp. 87-106.

H. Okabe, C. Caloz and T. Itoh; A Compact Enhanced-Bandwidth Hybrid Ring Using an Artificial Lumped-Element Left-Handed Transmission-Line Section, IEEE Trans. On Microwave Theory and Techniques, vol. 52, no. 3, march 2004, pp. 798-804, ISSN 0018-9480.

Caloz C., Dual Composite Right/Left-Handed (D-CRLH) Transmission Line Metamaterial, IEEE Microwave and Wireless Component Letters, vol. 16, no. 11, Nov. 2006, pp. 585-587, ISSN 1531-1309.

V.González-Posadas, J.L. Jiménez, L.E. García-Muñoz, D. Segovia-Vargas, Novel Diplexer Made with Dual-Composite Right/Left-Handed Lines (D-CRLH), Proceedings on the Czech and Slovak Microwave and Radioelectronics Week, april 2008, Prague.

J. Bonache, I. Gil, J. García-García, F. Martín; Complementary splits ring resonators for microstrip diplexer design, Electronic Letters, vol. 41, no. 14, Jul. 2005, pp. 810-811.

Y. Horii, C. Caloz, T. Itoh; Super-compact multilayered Left-handed transmission line and diplexer application, IEEE Trans. Microw. Theory Tech., vol. 53, no. 4, Apr. 2005, pp. 1527-1534, ISSN 0018-9480.

J.K.H. Wong, K.G. Balmain and G.V. Eleftheriades, A diplexer based on the spatial filtering property of planar anisotropic transmission-line metamaterials, Proceedings IMS MTT 2006.

F. J. Herraiz-Martínez, V. González-Posadas, F. Iñigo-Villacorta and D. Segovia-Vargas, Low-cost Approach based on an Eigenfrequency Method to obtain the Dispersion Diagram in CRLH Structures, IEEE Microwave and Wireless Components Letters, vol. 17, no.1, January 2007, pp. 13-15, ISSN 1531-1309.

C.-Y. Chang, and T. Itoh, Microwave active filters based on coupled negative resistance method, IEEE Trans. Microw. Theory Tech., vol. 38, no. 12, Dec. 1990, pp. 1879-1884, ISSN 0018-9480.

S. Lucyszyn, and I. D. Robertson, Monolithic narrow-band filter using ultrahigh-Q tunable active inductors, IEEE Trans. Microw. Theory Tech., vol. 42, no. 12, Dec. 1994, pp. 2617-2622, ISSN 0018-9480.

C. Rauscher, Microwave active filters based on transversal and recursive principles, IEEE Trans. Microw. Theory Tech., vol. 33, no. 12, Dec. 1985, pp. 1350-1360, , ISSN 0018-9480.

L. Billonnet, B. Jarry, and P. Guillon, Stability diagnosis of microwave recursive structures using the NDF methodology, IEEE MTT-S International Microw. Symp Dig., vol. 3, May 1995, pp. 1419-1422.

O. García-Pérez, A. García-Lampérez, V. González-Posadas, M. Salazar-Palma, D. Segovia-Vargas, Dual band recursive active filters with composite right/left handed transmission lines, IEEE Trans. Microw. Theory Tech., vol.57, no 5, May2009, pp.1180-1187, ISSN 0018-9480.

K.-K. M. Cheng and F. L. Wong, A novel approach to the design and implementation of dual-band compact planar 90º branch-line coupler, IEEE Trans. Microw. Theory Tech., vol. 52, no. 11, Nov. 2004, pp. 2458-2463, ISSN 0018-9480.

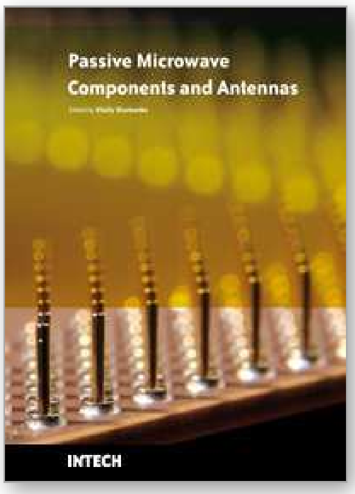

Passive Microwave Components and Antennas
Edited by Vitaliy Zhurbenko

ISBN 978-953-307-083-4
Hard cover, 556 pages
Publisher InTech
Published online 01, April, 2010
Published in print edition April, 2010

Modelling and computations in electromagnetics is a quite fast-growing research area. The recent interest in this field is caused by the increased demand for designing complex microwave components, modeling electromagnetic materials, and rapid increase in computational power for calculation of complex electromagnetic problems. The first part of this book is devoted to the advances in the analysis techniques such as method of moments, finite-difference time- domain method, boundary perturbation theory, Fourier analysis, mode-matching method, and analysis based on circuit theory. These techniques are considered with regard to several challenging technological applications such as those related to electrically large devices, scattering in layered structures, photonic crystals, and artificial materials. The second part of the book deals with waveguides, transmission lines and transitions. This includes microstrip lines (MSL), slot waveguides, substrate integrated waveguides (SIW), vertical transmission lines in multilayer media as well as MSL to SIW and MSL to slot line transitions.

InTech Europe
University Campus STeP Ri
Slavka Krautzeka 83/A
51000 Rijeka, Croatia
Phone: +385 (51) 770 447
Fax: +385 (51) 686 166
www.intechopen.com

InTech China
Unit 405, Office Block, Hotel Equatorial Shanghai
No.65, Yan An Road (West), Shanghai, 200040, China
中国上海市延安西路65号上海国际贵都大饭店办公楼405单元
Phone: +86-21-62489820
Fax: +86-21-62489821